

Spin interfaces in the Ashkin-Teller model and SLE

Y. Ikhlef¹ and M. A. Rajabpour^{2*}

¹ Section Mathématiques, Université de Genève
2-4 rue du Lièvre, CP 64, 1211 Genève 4, Switzerland

² SISSA and INFN, Sezione di Trieste, via Bonomea 265, 34136 Trieste, Italy

July 11, 2018

Abstract

We investigate the scaling properties of the spin interfaces in the Ashkin-Teller model. These interfaces are a very simple instance of lattice curves coexisting with a fluctuating degree of freedom, which renders the analytical determination of their exponents very difficult. One of our main findings is the construction of boundary conditions which ensure that the interface still satisfies the Markov property in this case. Then, using a novel technique based on the transfer matrix, we compute numerically the left-passage probability, and our results confirm that the spin interface is described by an SLE in the scaling limit. Moreover, at a particular point of the critical line, we describe a mapping of Ashkin-Teller model onto an integrable 19-vertex model, which, in turn, relates to an integrable dilute Brauer model.

Keywords: Ashkin-Teller Model, Critical interfaces, SLE.

PACS numbers: 05.50.+q, 11.25.Hf

1 Introduction

The scaling limit of interfaces in statistical models has attracted much attention since the early developments of conformal field theory (CFT). Starting from a local, classical spin model – *e.g.* the $O(n)$, Potts, \mathbb{Z}_N , XY models – there are essentially two ways of defining extended interfaces. One may consider the polygons in a graphical high-temperature expansion, *or* the spin interfaces (or domain walls) separating regions with different spin values.

As far as exact solutions are concerned, the situation turns out to be very different for these two kinds of interfaces. On one hand, in several models, including the $O(n)$ and Potts models, the high-temperature polygons are described by a Coulomb gas (CG) [1, 2], *i.e.* in the scaling limit, they become the level lines of a free compact boson CFT. Many geometric properties of these polygons can then be computed exactly through their mapping to correlation functions in this CFT. This yielded also solid conjectures (and, in some cases, rigorous proofs [3]) about their convergence to a Schramm-Loewner Evolution (SLE) model. On the other hand, despite some recent progress [4, 5], no consistent theory was identified as the scaling limit of spin interfaces, even in well-studied models such as the Potts model (except in the particular case of the Ising model), and very few scaling properties of these interfaces are actually known analytically.

*e-mail: rajabpour@sissa.it

Another current research direction is the study of “extended” SLEs, which are curve models determined by two random processes: the driving process of the Loewner chain, and an additional process corresponding, in the associated statistical model, to local variables which are *not* fixed locally by the presence of the curve. It was argued [6, 7] that the martingale conditions for this pair of processes correspond to null-state equations in an extended CFT. In particular, the presence of the additional process affects the relation between the central charge c and the SLE parameter κ . An important point that needs to be considered in this context, is that in the presence of additional variables, the lattice interface no longer satisfies the *Markov property*, which is an essential ingredient of the SLE model.

The Ashkin-Teller (AT) model is a simple local spin model, with a critical line of constant central charge $c = 1$ and varying exponents. We believe it presents the two features described above: first, although it has been much studied with both lattice and CFT techniques, the scaling theory for its spin interfaces is not identified, and second, these interfaces leave some fluctuating variables, which makes them good candidates for extended SLEs.

This paper presents two advances in the study of spin interfaces, on the particular example of the AT model. First, we introduce some specific boundary conditions (BCs) which ensure that the spin interface satisfies the Markov property, even in the presence of an additional variable. We then verify numerically that our interface relates to SLE, and for this purpose, we introduce a new algorithm allowing the measurement of the left-passage probability [8] in the transfer-matrix formalism. Our results also include an accurate numerical determination of the fractal dimension d_f of spin interfaces, also by means of the transfer matrix, which supports a conjecture for d_f stated in [9]. Second, we identify a specific value on the critical line of the AT model, where the temperature tends to zero, and at this point, we describe an exact mapping of the AT model onto an integrable 19-vertex model. Although this second result does not give direct access to spin interface exponents, this represents an alternative way of solving exactly the AT model, and may lead to additional exact results on this model.

2 Spin interfaces in the Ashkin-Teller model

The Ashkin-Teller model is a two-parameter model with a self-dual, critical line along which the central charge is constant $c = 1$ and the critical exponents vary. Its local correlation functions are described by the \mathbb{Z}_2 -orbifold of the compact boson CFT. However, like for the Potts model, this CG description only yields results for a specific class of interfaces, which does not include the spin DWs. A striking fact illustrating this is the absence of an exact result (except at specific values of the couplings) for the fractal dimension of spin DWs along the critical line!

To be more precise, let us summarize here the current knowledge on spin interfaces in the AT model. On the square lattice, the AT model consists of two spin variables σ_j and τ_j at each site j , taking the values ± 1 , and with the Boltzmann weight

$$W[\sigma, \tau] = \prod_{\langle ij \rangle} \exp [\beta(\sigma_i \sigma_j + \tau_i \tau_j) + \alpha \sigma_i \sigma_j \tau_i \tau_j] , \quad (1)$$

where the product is on all pairs of neighbouring sites. The critical line for the square lattice is given by the condition:

$$\sinh 2\beta = e^{-2\alpha} , \quad (2)$$

which we parametrize as

$$2 - \coth 2\beta = 1 - e^{4\alpha} = 2 \cos \pi g , \quad \text{with } 0 \leq g \leq 1. \quad (3)$$

To exhibit the \mathbb{Z}_4 invariance of the model, it is convenient to introduce the complex variables $S_j := \frac{\sigma_j - i\tau_j}{1-i}$, satisfying $S_j^4 = 1$, so that one can write (1) as

$$W[S] = \prod_{\langle ij \rangle} \exp \left\{ \beta(S_i^* S_j + S_j^* S_i) + \frac{\alpha}{2} [(S_i^* S_j)^2 + (S_j^* S_i)^2] \right\}. \quad (4)$$

This Boltzmann weight is invariant under the global rotation $S_j \rightarrow e^{\frac{i\pi}{2}} S_j$ and reflection $S_j \rightarrow S_j^*$. A non-branching spin interface in the AT model is specified by the partition into two sets of the four possible spin configurations (σ, τ) :

$$1 : (++) \quad 2 : (+-) \quad 3 : (--) \quad 4 : (-+). \quad (5)$$

For example, (14|23) denotes the interface between sites with values 1 or 4, and sites with values 2 or 3. The symmetries of (4) only leave three possible nonequivalent non-branching spin interfaces:

- The case (13|24) corresponds to domain walls for the variable $\tau' = \sigma\tau$. The associated operator has constant conformal dimension $h = \frac{1}{4}$ throughout the critical line, and hence the fractal dimension is $\frac{3}{2}$. In a previous work [10], we constructed a discrete holomorphic parafermion ψ_s of spin s in the AT model, which allowed us to relate the (13|24) interface to SLE(4, ρ, ρ), where the value of ρ was derived from the knowledge of s . The problem of the (13|24) interface with various boundary conditions was also addressed numerically in [11] and [12], yielding a set of conjectured relations to SLE(4, ρ', ρ'), and confirming the above results.
- The case (1|234) is not understood for general couplings, but for $g = 3/4$ (where the AT model coincides with the integrable Fateev-Zamolodchikov \mathbb{Z}_4 spin model), the associated operator satisfies a null-state equation in the \mathbb{Z}_4 -parafermionic CFT, and is argued [13] to have fractal dimension $\frac{17}{12}$.
- The case (12|34) corresponds to domain walls for the variable σ . Its fractal dimension is only known for a few values of the parameter g :

g	univ. class	d_f
1/4	O($n = 2$)	3/2
1/2	Ising	11/8
3/4	\mathbb{Z}_4 -parafermions	17/12
1	four-state Potts	3/2

The fractal dimension cannot be simply obtained from the CG analysis. However, based on the above exact values and Monte-Carlo simulations (in the region between Ising and Potts points), the following expression was proposed [9] for d_f :

$$d_f = \frac{7}{8} + \frac{g}{2} + \frac{1}{8g}. \quad (6)$$

3 Spin interface with the Markov property

3.1 Definition

Let Ω be a domain of the square lattice, and a and b two lattice sites on the boundary. We want to find boundary conditions (BCs) such that:

- Every spin configuration on Ω contains a (12|34) spin interface γ going from a to b . We denote the sites of the path γ as $(\gamma_0, \gamma_1, \dots, \gamma_\ell)$, where $\gamma_0 = a$, $\gamma_\ell = b$, and ℓ is the length of γ .
- The induced probability measure on γ satisfies the Markov property.

The *Markov property* for a probability measure $\mu_{\Omega, a, b}$ on paths means that, for any time s , the measure conditioned on $(\gamma_0, \dots, \gamma_s)$ is the same as the measure defined in $\Omega \setminus (\gamma_0, \dots, \gamma_s)$:

$$\forall s > 0, \quad \mu_{\Omega, a, b}(\cdot | \gamma_0, \dots, \gamma_s) = \mu_{\Omega \setminus (\gamma_0, \dots, \gamma_s), \gamma_s, b}(\cdot). \quad (7)$$

In other words, any piece of curve connected to the boundary should act like the boundary itself, when viewed from bulk variables.

Note that the BCs associated to a (12|34) spin interface – *i.e.* fixing the boundary spins to be in $\{1, 2\}$ on one side of the boundary between a and b and $\{3, 4\}$ on the other side – usually do not produce a Markov curve as soon as $\alpha \neq 0$. Indeed, conditioning on $(\gamma_0, \dots, \gamma_s)$ correctly fixes the σ spins on the boundary of $\Omega \setminus (\gamma_0, \dots, \gamma_s)$, but the resulting measure on spins includes interaction factors $-\alpha \tau_i \tau_j$ for neighbouring edges $\langle ij \rangle$ which cross $(\gamma_0, \dots, \gamma_s)$, and hence the conditioned measure on $(\gamma_s, \dots, \gamma_\ell)$ is *not* equal to the measure induced by the AT model on $\Omega \setminus (\gamma_0, \dots, \gamma_s)$. We thus need to introduce different BCs.

It is convenient to describe our BCs (see Fig. 1a) on an infinite strip of width L sites

$$S_L = \{(x, y), x \in \{1, \dots, L\}, y \in \mathbb{Z}\}.$$

Spins are fixed to be in $\{1, 2\}$ on the left boundary, and in $\{3, 4\}$ on the right boundary. The Boltzmann weights are defined as in (1), except that the product is now on neighbouring pairs $\langle ij \rangle$ of the *cylinder* of width L , *i.e.* it includes pairs of sites $\langle (1, y), (L, y) \rangle$. In other words, the BCs are such that the σ spins live on a strip, and the τ spins on a cylinder. This defines a Markov (12|34) interface on the strip S_L , since any piece of the interface connected to infinity acts exactly like a boundary.

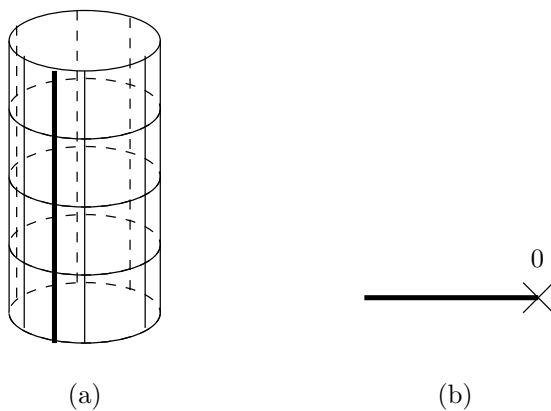


Figure 1: (a) Cylinder of circumference L sites. The thick line is a cut, such that adjacent spins on its right have values in $\{1, 2\}$, and adjacent spins on its left have values in $\{3, 4\}$. The Boltzmann weights include interactions along edges which cross the cut, so that the spins live on the cylinder, while the (12|34) interface lives on the strip. (b) The corresponding setting in the infinite plane: the domain for the interface is now the plane with a cut $\{z \in \mathbb{C} | z < 0\}$.

3.2 Scaling limit

The above definition may be adapted to any domain Ω formed by the complex plane with an infinite cut starting at the origin (see Fig. 1b): the spins are then fixed to $\{1, 2\}$ on one side of the cut, and to $\{3, 4\}$ on the other side, and we take the AT interaction of the full plane.

In the scaling limit, the spin interface is expected to become a continuous curve in Ω , with a conformally invariant distribution. Assuming that the Markov property is preserved in this limit, Schramm's principle tells us that the distribution of γ is SLE_κ , for some values of κ . In the case $g = 1/2$, γ is an Ising spin interface, and its relation to SLE_3 is proved rigorously [3].

Note that the above definition is restricted to a particular type of domains, namely those where the boundary consists in a cut, *i.e.* a possibly half-infinite simple curve. This is because we want to include interactions across the boundary, which automatically ensures the Markov property. Extending this idea to a generic simply-connected domain requires the introduction of a “gluing” map f associated to, (Ω, a, b) , that is a continuous bijection between the two arcs of the boundary defined by a and b . The measure should include an interaction between z and $f(z)$ for all points z on the boundary. For instance, in the SLE process, if we denote ${}_t$ the guiding process, f_t is a one-to-one mapping between $\{z < a_t\}$ and $\{z > a_t\}$, which is given by $f_0(z) = -z$ at the initial time $t = 0$, and evolves according to the Loewner process. The presence of the process f_t certainly affects the martingale conditions for correlation functions, which in turn modifies the relation between κ and the central charge. In particular, in the AT model, this accounts for the fact that the central charge remains constant $c = 1$, whereas κ varies as a function of g .

More formally, one now needs to consider a measure $\mu_{\Omega, a, b}$ on (γ, f) , and the Markov property reads

$$\mu_{\Omega, a, b}(f, \cdot | \gamma_{[0, t]}) = \mu_{\Omega \setminus \gamma_{[0, t]}, \gamma_{t, b}}(\tilde{f}^{(t)}, \cdot), \quad \text{where} \quad \tilde{f}^{(t)}(z) = \begin{cases} f(z) & \text{if } z \in \partial\Omega \\ z & \text{if } z \in \gamma_{[0, t]}. \end{cases} \quad (8)$$

Similarly, under a Loewner process g_t in the half-plane, the function f_t evolves as

$$f_t := g_t \circ \tilde{f}^{(t)} \circ g_t^{-1}, \quad (9)$$

where $\tilde{f}^{(t)}$ is defined in (8). Assuming that all the relevant information about fluctuating variables (in this case, the spins τ close to the boundary) is encoded in f_t , the Markov property (and the associated martingale conditions) should determine a non-standard relation between c and κ .

3.3 Numerical results

For generic g , we check numerically that the spin interface becomes an SLE in the scaling limit, using some known properties of SLE_κ . First, the fractal dimension of SLE_κ is given by

$$d_f = 1 + \frac{\kappa}{8}. \quad (10)$$

Also, the probability that γ passes to the left of a point (x, y) in the strip S_L is

$$P_{\text{left}}(x) = \frac{1}{2} - \frac{\Gamma(4/\kappa)}{\sqrt{\pi} \Gamma(\frac{8-\kappa}{2\kappa})} \cot\left(\frac{\pi x}{L}\right) {}_2F_1\left[\frac{1}{2}, \frac{4}{\kappa}, \frac{3}{2}, -\cot^2\left(\frac{\pi x}{L}\right)\right]. \quad (11)$$

In the lattice model, both d_f and P_{left} can be computed numerically by transfer-matrix diagonalisation, yielding two independent determinations of κ . The fractal dimension is obtained from the two-leg watermelon conformal dimension X_2 as $d_f = 2 - X_2$, where X_2 is given by the dominant

eigenvalue of the transfer matrix on the cylinder in the sector where two interfaces are forced to propagate along the cylinder. Moreover, we observe a better convergence when the model lives on the triangular lattice, so we chose this setting for the determination of d_f . The probability P_{left} is computed from the components of the dominant eigenvector of the transfer matrix on the strip, as described in the Appendix.

The results for d_f are shown in Fig. 2, and are in very good agreement with the conjecture (6), on a large portion of the critical line. Close to $g = 1$, marginal operators typically arise, and cause very strong finite-size effects, which explains the poorer convergence in this region. The validity of (6) in this region was already checked by Monte-Carlo simulations in [9].

For the computation of P_{left} , we use the value $g = 1/3$, where the associated model is simpler, and hence the space of states on which the transfer matrix acts has smaller dimension. The numerical results on P_{left} , and the corresponding estimate of κ , are shown in Fig. 3 and Table 1. They match closely with the results on d_f , which is a strong indication that the curve distribution is $\text{SLE}_{\kappa=10/3}$.

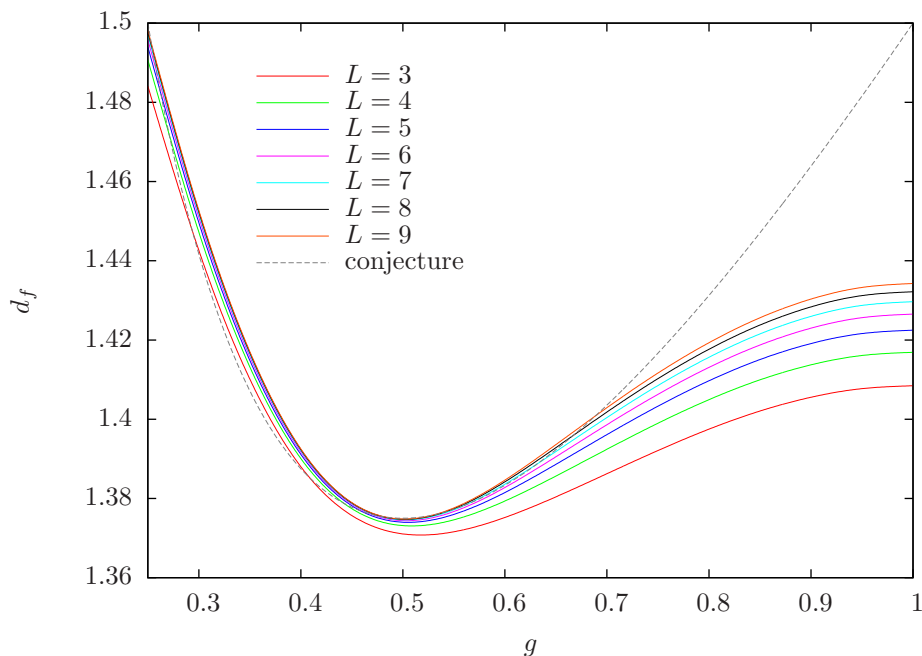


Figure 2: (Color online) Numerical determination of the fractal dimension d_f for the (12|34) interface in the triangular-lattice AT model. The dotted curve represents the conjectured value (6).

4 The zero-temperature point

The value $g = 1/3$ on the self-dual line (3) corresponds to the limit

$$\alpha \rightarrow -\infty, \quad \beta \rightarrow \infty, \quad e^{\alpha+\beta} = \sqrt{2}.$$

The Boltzmann weights then take the form

$$e^{-(2\beta+\alpha)\mathcal{N}} W[\sigma, \tau] = \prod_{\langle ij \rangle} \left[\delta_{\sigma_i, \sigma_j} \delta_{\tau_i, \tau_j} + \frac{1}{2} \delta_{\sigma_i, \sigma_j} (1 - \delta_{\tau_i, \tau_j}) + \frac{1}{2} (1 - \delta_{\sigma_i, \sigma_j}) \delta_{\tau_i, \tau_j} \right], \quad (12)$$

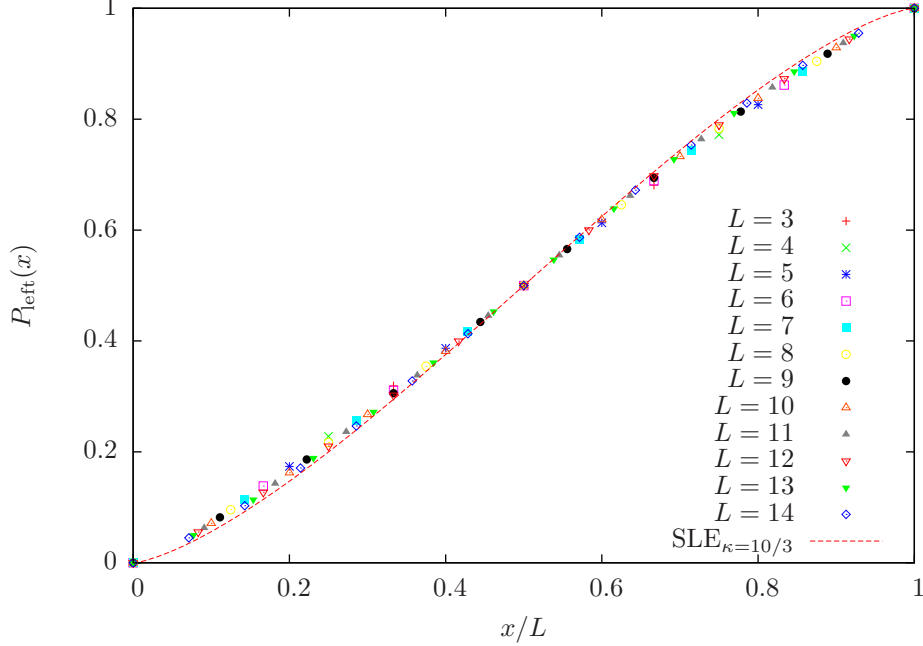


Figure 3: (Color online) Numerical determination of the left-passage probability P_{left} in the AT model for $g = 1/3$. The full line represents Schramm's formula, with the value $\kappa = 10/3$ from the conjecture (6).

where \mathcal{N} is the number of edges in Ω . The corresponding σ and τ domain walls thus form a two-colour loop model on the dual lattice, where a black (resp. gray) loop represents a σ (resp. τ) domain wall. Each edge of the dual lattice bears at most one colour of loop, and the weight of a loop configuration is K^ℓ , where $K = 1/2$, and ℓ is the total length of the loops. For completeness, we depict in Fig. 4 all the possible loop configurations around a vertex.

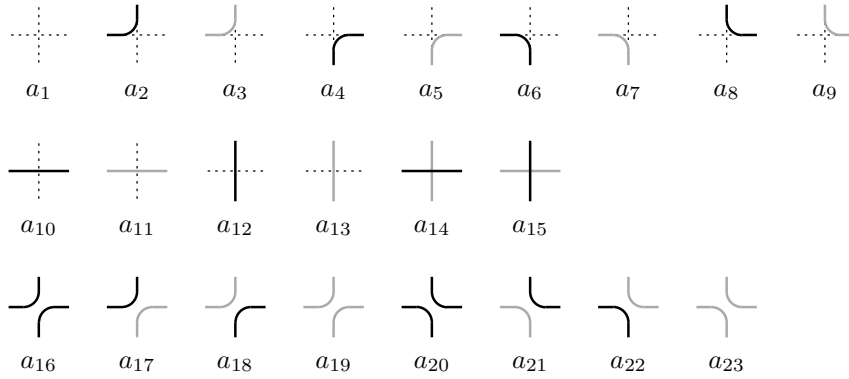


Figure 4: Vertices of the two-colour loop model.

Let us now expose an exact equivalence of this two-colour loop model of AT spin interfaces with an integrable 19-vertex (19V) model. As a first stage, we map the 19V model onto a dilute Brauer model with loop weight $n = 2$. The vertices of the latter model are shown in Fig. 5. Each of the Brauer loops can be oriented clockwise or anti-clockwise independently: this leads to a 19V model

L	κ
3	3.74332
4	3.70126
5	3.66359
6	3.62997
7	3.59999
8	3.57317
9	3.54905
10	3.52724
11	3.50738
12	3.48919
13	3.47295
14	3.45693

Table 1: Numerical estimates of κ from the left-passage probability P_{left} for $g = 1/3$ (see data in Fig. 3).

with weights

$$\omega_1 = t \tag{13}$$

$$\omega_2 = \omega_3 = \omega_4 = \omega_5 = u_1 \tag{14}$$

$$\omega_6 = \omega_7 = \omega_8 = \omega_9 = u_2 \tag{15}$$

$$\omega_{10} = \omega_{11} = \omega_{12} = \omega_{13} = v \tag{16}$$

$$\omega_{14} = \omega_{15} = w_1 + x \tag{17}$$

$$\omega_{16} = \omega_{17} = w_2 + x \tag{18}$$

$$\omega_{18} = \omega_{19} = w_1 + w_2, \tag{19}$$

where we have used the standard notations $(\omega_1, \dots, \omega_{19})$ as in [14]. If we take the FZ integrable weights [14] of the 19V, we obtain the dilute Brauer weights:

$$\begin{aligned}
t &= \sin \mu \sin 2\mu - \sin u \sin(\mu - u) \\
u_1 &= \sin 2\mu \sin(\mu - u) \\
u_2 &= \sin 2\mu \sin u \\
v &= \sin u \sin(\mu - u) \\
w_1 &= \sin 2\mu \sin(\mu - u) \cos u \\
w_2 &= \sin 2\mu \sin u \cos(\mu - u) \\
x &= -\cos 2\mu \sin u \sin(\mu - u).
\end{aligned} \tag{20}$$

It turns out that setting $\mu = \frac{2\pi}{3}$ and $u = \mu/2$, and letting $v \rightarrow -v$ (because v configurations always appear in even number) yields

$$\begin{aligned}
t &= 1 \\
u_1 = u_2 = v &= K \\
w_1 = w_2 &= K^2 \\
x &= -K^2.
\end{aligned} \tag{21}$$

The dilute Brauer model is, in turn, mapped to our two-colour loop model in the following way. Each of the Brauer loops can be coloured black or gray independently. Then, consider a vertex

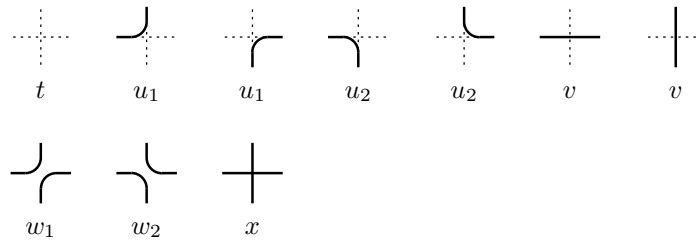


Figure 5: Vertices of the dilute Brauer model.

whose four adjacent edges bear the same colour. Since the coloured loops have weight unity, the overall Boltzmann weight of the configuration is the same for vertices w_1, w_2 and x . Thus the dilute Brauer model is equivalent to the two-colour loop model provided the following relations hold

$$\begin{aligned}
 a_1 &= t \\
 a_2 = \dots = a_5 &= u_1 \\
 a_6 = \dots = a_9 &= u_2 \\
 a_{10} = \dots = a_{13} &= v \\
 a_{14} = a_{15} &= \pm x \\
 a_{16} + a_{20} = w_{19} + w_{23} &= w_1 + w_2 + x \\
 a_{17} = a_{18} &= w_1 \\
 a_{21} = a_{22} &= w_2
 \end{aligned} \tag{22}$$

The integrable weights (21) satisfy these relations, and hence we have proved the equivalence.

For the parameters $\mu = \frac{2\pi}{3}$ and $u = \mu/2$, the 19V model is described [16] in the continuum limit by a $c = 1$ compact boson CFT with the spectrum of conformal dimensions

$$x_{n,m} = \frac{\mu}{2\pi}n^2 + \frac{\pi}{2\mu}m^2, \quad n, m \in \mathbb{Z}^2. \tag{23}$$

It turns out that the excitations described by this spectrum describes are not directly related to those of the colored loops. In particular, they do not include the conjectured two-leg exponent $x_2 = 7/12$. However, the mapping to a 19V model may be exploited to obtain new exact results on the AT model at zero temperature.

5 Conclusion

In the present work, we have presented a set of new results on spin interfaces in the AT model.

By a numerical study based on transfer-matrix diagonalisation, we have given a precise numerical determination of the fractal dimension d_f , in a parameter regime that could not be accessed previously by a Monte-Carlo simulation [9]. Our results on d_f bring more support to the conjectural expression (6) introduced in [9]. Moreover, we have shown, for the first time, how to adapt the transfer-matrix method to measure numerically the left-passage probability P_{left} , which is a natural quantity in the SLE literature.

On the analytical side, we introduce a general way of choosing BCs which preserve the discrete Markov property of a path, even in the presence of additional degrees of freedom which are not fixed locally by the path. This construction is quite general, and may be extended to any lattice model with interfaces of this sort. The left-passage probability P_{left} is then computed numerically

with these “Markovian” BCs, and the results for P_{eff} confirm that the resulting measure on curves becomes SLE in the continuum limit.

We have also identified a specific point on the critical line of the AT model, the point where all the couplings diverge, where there is a mapping of the AT model onto an integrable 19-vertex model. At this point the interfaces of the σ and τ spins live in different bonds and so the corresponding two-color loop model has a simpler form. At this particular point one can also find a dilute Brauer model representation of the critical spin interfaces of the AT model. Since the loop model has a simpler form at this particular point, we believe it is a good place to look for a Coulomb gas representation of the AT spin interfaces, and extend it to the critical line afterwards.

Our work presents conclusive numerical arguments that the spin interfaces in AT model are conformally invariant and their fractal dimension follow the formula (6), motivating further the search for an analytic argument which would account for (6). This is a simple example of the more general notion of spin interfaces, for which very few analytical results are available. On top of the recent methods for the study of lattice models, like discrete holomorphic parafermions, our construction of “Markovian” BCs seems an interesting starting point for this search.

Appendix: transfer-matrix algorithm for the left-passage probability

In this Appendix, we present a numerical procedure for the computation of the left-passage probability in a loop model defined on the infinite strip of width L sites. Let us describe how our method works on a simple loop model, such as the square-lattice $O(n)$ loop model (defined by the vertices in Fig. 5, with $x = 0$). The generalization to other loop models, such as the two-colour loop model studied in this paper, is straightforward.

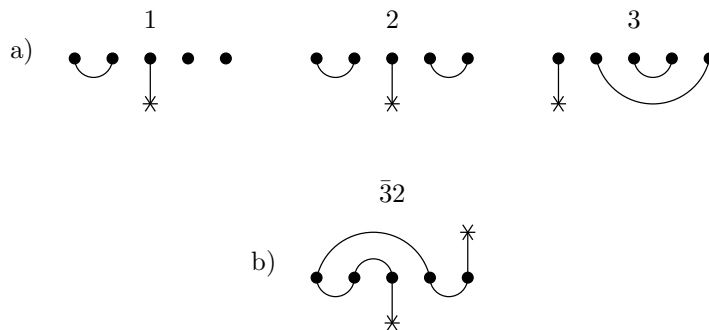


Figure 6: a) Some basis elements for $L = 5$. b) An example of the gluing operation involved in the definition of $\langle \cdot, \cdot \rangle$.

The basis elements α generating the space of states V_L are labelled by planar pairings of the points $\{1, \dots, L\}$, with one point paired with \star , as depicted in Fig. 6. The space V_L is also equipped with a scalar product $\langle \cdot, \cdot \rangle$, defined as follows. We say that two pairings α, β are compatible if they have the same subset of paired points, and we denote $\bar{\alpha}\beta$ the figure obtained by gluing the π -rotation of α to β . Then

$$\langle \alpha, \beta \rangle := \begin{cases} n^{\#\text{closed loops in } \bar{\alpha}\beta} & \text{if } \alpha \text{ and } \beta \text{ are compatible,} \\ 0 & \text{otherwise.} \end{cases} \quad (24)$$

Let us recall briefly how the transfer matrix T acts on V_L [15]. We take the convention that T acts from bottom to top, and adds one row to the system. When starting from a pairing configuration $|\beta\rangle$, the addition of one row gives rise to a linear combination of pairings $\sum_{\alpha} T_{\alpha\beta}|\alpha\rangle$, where the matrix element $T_{\alpha\beta}$ is given by the product of Boltzmann weights inside the row, including a factor n for each loop that got closed in the process.

We denote the dominant eigenstate of T in the sector with a propagating path as

$$|\psi\rangle = \sum_{\alpha} \psi_{\alpha} |\alpha\rangle. \quad (25)$$

If we cut the system into two half-infinite strips above and below a given horizontal section, then the L dangling edges of the top half have a pairing $\bar{\alpha}$, and those of the bottom half have a pairing β . If we assume that the local Boltzmann weights in T are invariant under a rotation of angle π , then the probability of a pair $(\bar{\alpha}, \beta)$ is

$$\mathbb{P}(\bar{\alpha}, \beta) = \frac{\psi_{\bar{\alpha}} \psi_{\beta} \langle \bar{\alpha}, \beta \rangle}{Z}, \quad \text{where} \quad Z = \sum_{\alpha, \beta} \psi_{\alpha} \psi_{\beta} \langle \alpha, \beta \rangle \quad (26)$$

For any pair $(\bar{\alpha}, \beta)$, we denote $\gamma_{\bar{\alpha}, \beta}$ the open path appearing in $\bar{\alpha}\beta$. For a given position $j \in \{0, \dots, L\}$, we introduce the modified scalar product $\langle \cdot, \cdot \rangle_j$:

$$\langle \alpha, \beta \rangle_j := \begin{cases} n^{\#\text{closed loops in } \bar{\alpha}\beta} & \text{if } \alpha \text{ and } \beta \text{ are compatible and } \gamma_{\bar{\alpha}, \beta} \text{ passes between } 0 \text{ and } j, \\ 0 & \text{otherwise.} \end{cases} \quad (27)$$

This allows us to express the left-passage probability P_{left} as

$$P_{\text{left}}(j) = \frac{1}{Z} \sum_{\alpha, \beta} \psi_{\alpha} \psi_{\beta} \langle \alpha, \beta \rangle_j. \quad (28)$$

Our method consists in the following steps

1. Determine the eigenstate (25) by the power method (iteration of T on a random initial vector).
2. Compute (28) by performing the double sum on configurations.

Since the computation of $\langle \alpha, \beta \rangle_j$ takes $O(L)$ operation, the overall complexity of step 2 is $O[L(\dim V_L)^2]$. The cost in memory is $O(\dim V_L)$, since only a finite number of vectors are stored in memory, as usual in transfer-matrix algorithms.

References

- [1] B. Nienhuis, *J. Stat. Phys.* **34** (1984) 731
- [2] P. di Francesco, H. Saleur and J. B. Zuber, *J. Stat. Phys.* **49** (1987) 57
- [3] S. Smirnov, *C. R. Acad. Sci. Paris* **333** (2001) 239;
S. Smirnov, *Conformal invariance in random cluster models: I. Holomorphic fermions in the Ising model*, [arXiv:0708.0039](https://arxiv.org/abs/0708.0039);
D. Chelkak and S. Smirnov, *Universality in the 2D Ising model and conformal invariance of fermionic observables*, [arXiv:0910.2045](https://arxiv.org/abs/0910.2045)

- [4] A. Gamsa and J. Cardy, *J. Stat. Mech.* (2007) P08020
- [5] J. Dubail, J. L. Jacobsen and H. Saleur, *J. Phys. A* **43** (2010) 482002
- [6] E. Bettelheim, I. A. Gruzberg, A. W. W. Ludwig and P. Wiegmann, *Phys. Rev. Lett.* **95** (2005) 251601
- [7] R. Santachiara, *Nucl. Phys. B* **793** (2008) 396
- [8] O. Schramm, *Electronic Comm. Probab.* **8** (2001), paper no. 12
- [9] M. Caselle, S. Lottini and M. A. Rajabpour, *J. Stat. Mech.* **1102** (2011) P02039
- [10] Y. Ikhlef and M. A. Rajabpour, *J. Phys. A* **44** (2011) 042001
- [11] M. Picco, R. Santachiara, *Phys. Rev. E* **83** (2011) 061124
- [12] D. Wilson, *XOR-Ising Loops and the Gaussian Free Field*, [arXiv:1102.3782](https://arxiv.org/abs/1102.3782)
- [13] M. Picco and R. Santachiara, *J. Stat. Mech.* **1007** (2010) P07027
- [14] B. Nienhuis, *Int. J. Mod. Phys. B* **4** (1990) 929
- [15] H. W. J. Blöte and B. Nienhuis, *J. Phys. A* **22** (1989) 1415
- [16] F. C. Alcaraz and M. J. Martins, *Phys. Rev. Lett.* **63** (1989) 708